THE JOURNAL OF BIOLOGICAL CHEMISTRY VOL. 288, NO. 10, pp. 7271–7281, March 8, 2013

Identification and Characterization of a Type III Polyketide Synthase Involved in Quinolone Alkaloid Biosynthesis from *Aegle marmelos* Correa*

Received for publication, October 24, 2012, and in revised form, January 16, 2013 Published, JBC Papers in Press, January 17, 2013, DOI 10.1074/jbc.M112.429886

Mohankumar Saraladevi Resmi[‡], Priyanka Verma[§], Rajesh S. Gokhale[§¶], and Eppurathu Vasudevan Soniya[‡1]

From the [‡]Plant Molecular Biology Division, Rajiv Gandhi Centre for Biotechnology, Thycaud (P.O), Thiruvananthapuram, 695 014 Kerala, India, the [§]National Institute of Immunology, Aruna Asaf Ali Marg, New Delhi 110067, India, and the [¶]Systems Biology Group, Council of Scientific and Industrial Research, Institute of Genomics and Integrative Biology, Mall Road, Delhi 110 007, India

Background: Type III polyketide synthase is hypothesized to produce quinolones, but no such enzyme has been identified so far.
Results: QNS, a type III PKS from *Aegle marmelos* synthesizes diketide 4-hydroxy-1-methyl-2*H*-quinolone using a unique substrate binding site.
Conclusion: QNS is a novel 4-hydroxy-1-methyl-2*H*-quinolone synthase.
Significance: This is the first report of a gene involved in quinolone biosynthesis from plants.

Quinolone alkaloids, found abundantly in the roots of bael (*Aegle marmelos*), possess various biological activities and have recently gained attention as potential lead molecules for novel drug designing. Here, we report the characterization of a novel Type III polyketide synthase, quinolone synthase (QNS), from *A. marmelos* that is involved in the biosynthesis of quinolone alkaloid. Using homology-based structural modeling, we identify two crucial amino acid residues (Ser-132 and Ala-133) at the putative QNS active site. Substitution of Ser-132 to Thr and Ala-133 to Ser apparently constricted the active site cavity resulting in production of naringenin chalcone from *p*-coumaroyl-CoA. Measurement of steady-state kinetic parameters demonstrates that the catalytic efficiency of QNS was several-fold higher for larger acyl-coenzymeA substrates as compared with smaller precursors. Our mutagenic studies suggest that this protein might have evolved from an evolutionarily related member of chalcone synthase superfamily by mere substitution of two active site residues. The identification and characterization of QNS offers a promising target for gene manipulation studies toward the production of novel alkaloid scaffolds.

Quinolones are anthranilic acid-derived alkaloids that are largely or completely restricted to plants of Rutaceae (1). Some of these naturally occurring quinolones have profound medicinal properties, whereas others have served as lead structures and provided inspiration for the design of synthetic quinolones as useful drugs (2, 3). Quinoline alkaloids such as quinine, chloroquin, mefloquine, and amodiaquine are used as efficient drugs for the treatment of malaria (4). Skimmianine is a potential quinolone alkaloid derived from the roots of many rutacean plants and is reported to possess various biological activities such as inhibitory effect on spontaneous motor function (5), cardiovascular effect (6), antiplatelet aggregation activity (7), cytotoxic in HeLa cell line (8), and also as antagonists of 5-hydroxytryptamine receptors (9). Because of these properties, quinolone biosynthesis is a subject of great interest. Recently, a report by Abe *et al.* (10) demonstrated the ability of benzalacetone synthase (BAS),[2] a type III PKS to accept non-physiological substrate *N*-methylanthraniloyl CoA and catalyze formation of 4-hydroxy-2(1*H*)-quinolones. However, until now, no type III PKS dedicated to biosynthesis of quinolone alkaloid has been identified. In this report, we characterize a novel type III PKS from *Aegle marmelos* Corr. and demonstrate its remarkable ability to catalyze formation of quinolones scaffold. Strikingly, *A. marmelos* Correa belongs to the Rutaceae family, which is widely recognized for the diversity of the associated quinolone alkaloid (11, 12).

Type III polyketide synthases (PKS) are homodimeric enzymes where the single active site in each monomer iteratively catalyzes the priming, extension, and cyclization reactions to generate the polyketide product. Despite their structural simplicity, type III PKS produces a variety of compounds, including pyrones, resorcinols, acridones, chalcones, stilbenes, and phloroglucinols (13, 14). The diversity observed with type III PKS arises from its ability to accept variety of acyl-CoA thioesters for priming the reaction, its capability to extend this starter with variable number of extender units and also perform different cyclizations of the poly-β-keto linear polyketide intermediate. Although type III PKS have been studied in plants for decades, genome sequencing projects has resulted in identification of type III PKS homologues from several bacteria, fungi, and lower eukaryotes (15). Interestingly, the first report of a type III PKS accepting long chain acyl-CoA substrates was reported from a bacterium, *Mycobacterium tuberculosis* (16).

* This work was supported by Department of Science and Technology, New Delhi, India, and a senior research fellowship from Council of Scientific and Industrial Research (New Delhi, India).

[1] To whom correspondence should be addressed: Plant Molecular Biology Div., Rajiv Gandhi Centre for Biotechnology, Thycaud(P.O), Thiruvananthapuram, 695 014 Kerala, India. Tel.: 91-471-252-9454; Fax: 91-471-234-8096; E-mail: evsoniya@rgcb.res.in.

[2] The abbreviations used are: BAS, benzalacetone synthase; PKS, polyketide synthase(s); QNS, quinolone synthase; RACE, rapid amplification of cDNA ends; ACS, acridone synthase.

In this report, we describe cloning and characterization of a novel type III PKS from *A. marmelos*, which is named quinolone synthase (QNS) on the basis of its activity. The reaction involves decarboxylative condensation of malonyl-CoA with *N*-methylanthraniloyl-CoA to form an intermediate, which spontaneously cyclize by amide formation to yield 4-hydroxy-2(1*H*)-quinolone. Kinetic analysis indicated that the catalytic efficiency of QNS protein to accept larger acyl-CoA substrate is severalfold higher than that for smaller substrates. Molecular modeling studies suggested that QNS might have emerged by the gain of function (by the substitution of simply two active site residues) mutation from a structurally homologous CHS type III protein. The catalytic and structural importance of active site residues, as predicted by our structural model, was investigated by performing site-directed mutagenesis. The modeling and mutagenesis studies provide an insight into the structural mechanism for the enzyme that could be used to generate pharmaceutically important products.

EXPERIMENTAL PROCEDURES

Materials—[2-^{14}C]Malonyl-CoA (58.40 mCi/mmol) was purchased from PerkinElmer Life Sciences, and nonradioactive acyl-CoA starter substrates such as malonyl-CoA, n-butyryl-CoA, isovaleryl-CoA, *n*-hexanoyl-CoA, benzoyl CoA, naringenin, 4-hydroxy 1-methyl quinolone, and *p*-hydroxy-benzalacetone were purchased from Sigma. *p*-Coumaroyl-CoA, feruloyl-CoA, and *N*-methylanthraniloyl-CoA were purchased from TransMIT.

Cloning, Expression, and Purification of QNS—5′ and 3′ RACE experiments using gene-specific primers were performed for obtaining the full-length cDNA of QNS from RNA prepared using First Choice RNA Ligase Mediated RACE kit (Ambion) as per manufacturer's protocol. For 3′ RACE, 5′-TAGTGGGTCAGGCTCTTTTTGC-3′ and 5′-GCATCCATTGAGCGTCCATTGT-3′ and for 5′ RACE, 5′-AATGAACTGTTAGACCCGCCTC-3′ and 5′-CCATCAGAATCAGGCAGAAGCG-3′ were used along with adaptor specific primers provided with the kit. Full-length QNS was isolated using forward primer, 5′-ATGGTAACCATGGAGGAGATTAGA-3′ and reverse primer, 5′-TCAAGCTTCGATGGGGACACTGCG-3′. Using the full-length information, QNS was also amplified from genomic DNA using the same primers for full-length QNS cDNA amplification. The QNS was expressed in the prokaryotic system as a fusion protein with His_6 tag using the expression vector of the series pET32 (Novagen). QNS was in-frame cloned into the EcoRI site of pET32b vector and was transformed into competent *Escherichia coli* BL21(DE3) cells. The inducibility was monitored at regular interval of 1 h in presence of 0.4 mM isopropyl-1-thio-β-galactopyranoside and confirmed by Western blotting using anti-His tag antibody. For the purification of protein, the transformed BL21(DE3) cells were grown to $A_{600} = 0.5$ and induced in 0.4 mM isopropyl-1-thio-β-galactopyranoside at 28 °C for 6 h. The bacterial pellet was then resuspended in protein buffer A (50 mM KPO_4 buffer, pH 8.0, 100 mM NaCl, 0.7 mg/ml lysosyme, 40 mM imidazole) and sonicated in ice at 50% duty cycle at intermediate power. The lysate was analyzed by SDS-PAGE and subjected to nickel-nitrilotriacetic acid-agarose column chromatography (Invitrogen). After washing with protein buffer B (50 mM KPO_4 buffer, pH 7.9, 500 mM NaCl, and 40 mM imidazole), QNS was eluted with protein buffer C (15 mM KPO_4 buffer, pH 7.5, 150 mM imidazole, and 10% glycerol) and analyzed by SDS-PAGE.

Site-directed Mutagenesis—*A. marmelos* QNS mutants MSD1 and MSD2 were constructed using the QuikChange site-directed mutagenesis kit (Stratagene) and a pair of primers as follows (mutated codons are *underlined*): MSD1 (S132T/A133S) (5′-CTCATTTTCTGCACAACTTCAGGCGTCGACATG-3′ and 5′-CATGTCGACGCCTGAAGTTGTGCAGAAAATGAG-3′)) and MSD2 (V265F in addition to S132T/A133S) (5′)-GAGGCGGGTCTAACATTTCATTTGAAGAAAGAC-3′ and 5′-GTCTTTCTTCAAATGAAATGTTAGACCCGCCTC- 3′). Mutagenesis was confirmed by automated DNA sequencing. The mutant proteins were expressed and tried to purify analogous to the wild-type QNS protein. The mutants expressed as inclusion bodies and could not be expressed in soluble form when similar conditions as wild-type QNS protein were used. The expression of mutant protein was modulated to soluble form by inducing cultures with 0.4 mM isopropyl-1-thio-β-D-galactopyranoside concentration at 18 °C for 24 h.

Enzyme Assay and Product Characterization Using Mass Spectrometry—For the *in vitro* enzyme assay, the standard reaction conditions involved 200 μM starter molecule (*n*-butyryl-CoA, isovaleryl-CoA, *n*-hexanoyl-CoA, benzoyl-CoA, cinnamoyl-CoA, *p*-coumaroyl-CoA, feruloyl-CoA, and *N*-methylanthraniloyl-CoA) and 100 μM malonyl-CoA (inclusive of 9.12 μM [2-^{14}C]malonyl-CoA (58.40 mCi/mmol)). Reactions were carried out with 45 μg of protein at 30 °C for 60 min and quenched with 5% acetic acid. The products were extracted with 2 × 300 μl of ethyl acetate and dried under vacuum. Radiolabeled products were resolved on silica gel 60 F_{254} TLC plates (Merck) in ethyl acetate/hexanes/acetic acid (63:27:5, v/v/v). Polyketide products were characterized using nanospray electrospray ionization MS (API QSTAR Pulsar i MS/MS; Applied Biosystems).

Determination of the Kinetic Parameters—A standard reaction contained 100 mM potassium phosphate buffer (pH 7.0), 200 μM malonyl-CoA, *N*-methylanthraniloyl-CoA (0.5–200 μM), and 40 μg of QNS in a total volume of 100 μl for determination of kinetic values for *N*-methylanthraniloyl-CoA, and 100 mM potassium phosphate buffer (pH 7.0), 200 μM malonyl-CoA, varied starter concentrations (2.5–200 μM), and 40 μg of QNS in a total volume of 100 μl for determination of kinetic values for all other starter CoAs. After the reaction mixture had been preincubated at 37 °C for 2 min, reactions were initiated by adding the substrate and continued for 20 min. The reactions were stopped with 5 μl of 5% acetic acid, and the material in the mixture was extracted with 2× ethyl acetate. The organic layer was collected and evaporated. The residual materials were dissolved in 20 μl of methanol for Radio-TLC analysis. The kinetic parameters were calculated for formation of major product of the enzyme reactions.

Homology Modeling and Docking Studies—Structural modeling was done based on the homology using the SWISS-MODEL workspace (17–19), which is an integrated web-based modeling expert system. To get the suitable template for QNS,

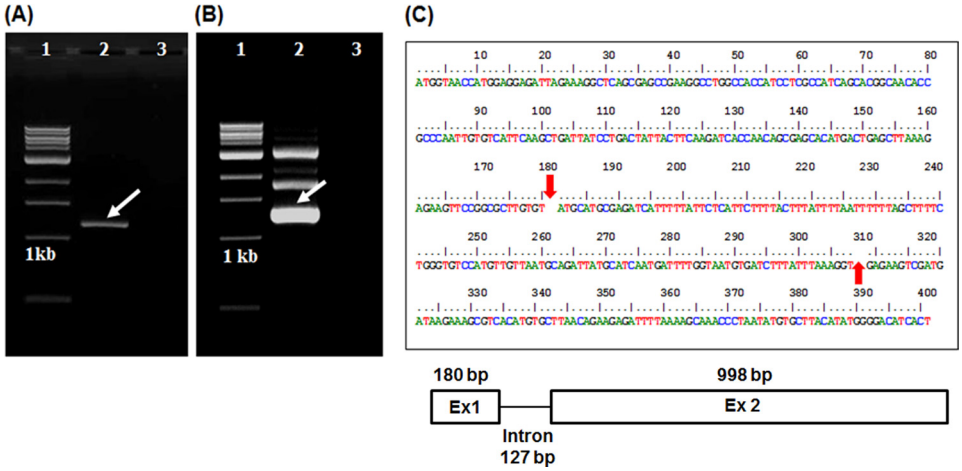

FIGURE 1. **Amplification of QNS from *A. marmelos* leaves.** *A* and *B*, PCR amplification of QNS from cDNA ad genomic DNA, respectively. *1*, 1-kb DNA ladder; *2*, PCR product; *3*, control reaction. *C*, organization of intron in QNS gene. The *arrow* indicates the predicted intron position. The diagrammatic representation of QNS genome organization was also shown below.

we did Blastp search (www.ncbi.nlm.nih.gov/blast) against the Protein Data Bank using an E value cut-off: 0.001. Based on the result *Medicago sativa* CHS (Protein Data Bank code 1BI5, chain A; resolution, 1.56; 74% identity) was selected as template. Calculation of cavity volumes (Connolly's surface volumes) was then performed with the CASTP program (available online) (20). To find out the preferred substrates for the enzyme, we tried to dock substrate molecules like *p*-coumaroyl-CoA and *N*-methylanthraniloyl-CoA to the QNS wild-type and mutant proteins. For docking studies, HEX (version 4.5, 21) was used with default parameters. The substrates were obtained from PubChem database.

RESULTS

Sequence Analysis and Homology Modeling—The full-length cDNA of ~1200 bp (Fig. 1*A*) was obtained from young leaves of *A. marmelos* via amplification through RNA Ligase Mediates RACE experiments (the details of the method are described under "Experimental Procedures"). To study the genomic organization of QNS, the full-length gene was also isolated and cloned from *A. marmelos* genomic DNA, which was ~1305 bp in length (GenBank ID, JX679860) (Fig. 1*B*). The sequencing results showed that the coding region of QNS is interrupted by one intervening sequence of 127 bp (Fig. 1*C*) as reported in almost all plant-specific type III PKS genes (22–24) that is located between the first and second nucleotides of Cys-60-encoding triplet (numbering of *M. sativa* CHS2). The primary cDNA sequence of *A. marmelos* QNS (GenBank ID JX679859) exhibits 60–75% identity to CHS superfamily enzymes from other plant species, including *M. sativa* CHS and *Gerbera hybrida* 2-PS. The closest homologue to QNS is chalcone synthase from *Dictamus albus* (81% amino acid identity) and acridone synthase (ACS) from *Ruta graveolens* (79% amino acid identity). An alignment was made, and a phylogenetic tree was constructed with others type III PKS in the database, including the highly homologous ones to study the evolutionary relationship of QNS (Fig. 2, *A* and *B*). Phylogenetic analysis revealed that QNS groups with non-chalcone forming PKS and cluster with *R. graveolens* ACS (Fig. 2*B*). Comparative analysis of protein sequences of plants PKS superfamily of enzymes have previously led to the clustering of these proteins based on their function and not based on species-specific nature (25, 26). *A. marmelos* QNS maintains an almost identical CoA binding site with the reported type III PKS and a conserved catalytic triad of Cys-164, His-303, and Asn-336 (numbering in *M. sativa* CHS) (Table 1). In addition, the active site residues, including Leu-214, Ile-254, Gly-256, Thr-197, Leu-263, and Ser-338 of *M. sativa* CHS are well conserved in QNS (Table 1). Strikingly, *A. marmelos* QNS lacks active site Phe-265, the second "gatekeeper Phe" in type III PKS of plant and bacterial origin and is replaced by Val-265. Additionally the active site residues, Thr-132 and Ser-133 of *M. sativa* CHS are replaced by Ser-132 and Ala-133 residues (Table 1). Similar type of T132S, S133A, and F265V substitutions are present in both ACS isoforms from *R. graveolens* and are reported to play key role in starter substrate specificity (27).

Structure-based homology modeling and docking studies were carried out to get an insight into the role of active site residues in QNS substrate binding activity. Homology models of QNS wild-type and mutants, MSD1 (S132T/A133S), and MSD2 (S132T/A133S/V265F) were generated based on *M. sativa* CHS (Protein Data Bank code 1BI5) as template (Fig. 3). The homology model of *A. marmelos* QNS wild-type showed that it has the same overall fold as *M. sativa* CHS, with cavity volume estimated to be 1196 $Å^3$, which is much larger than that of *M. sativa* CHS (1019 $Å^3$). This also suggested that the active site cavity of QNS is easily large enough to accommodate bulkier starter substrate than CHS. The three residues Ser-132, Ala-133, and Val-265 lie near or line the active cavity. The mutant MSD1 and MSD2 homology models shows remarkable constriction in the active site cavity with a volume estimated to be 1188 and 1168 $Å^3$, respectively (Fig. 3). We therefore predicted that the steric bulk from three active site residues substitution, S132T, A133S, and V265F, in mutants significantly affect the active site volume and might hinder the binding of bulkier starter substrates in mutants. To improve our predictability for MSD1 and MSD2 mutants, *N*-methylanthraniloyl-

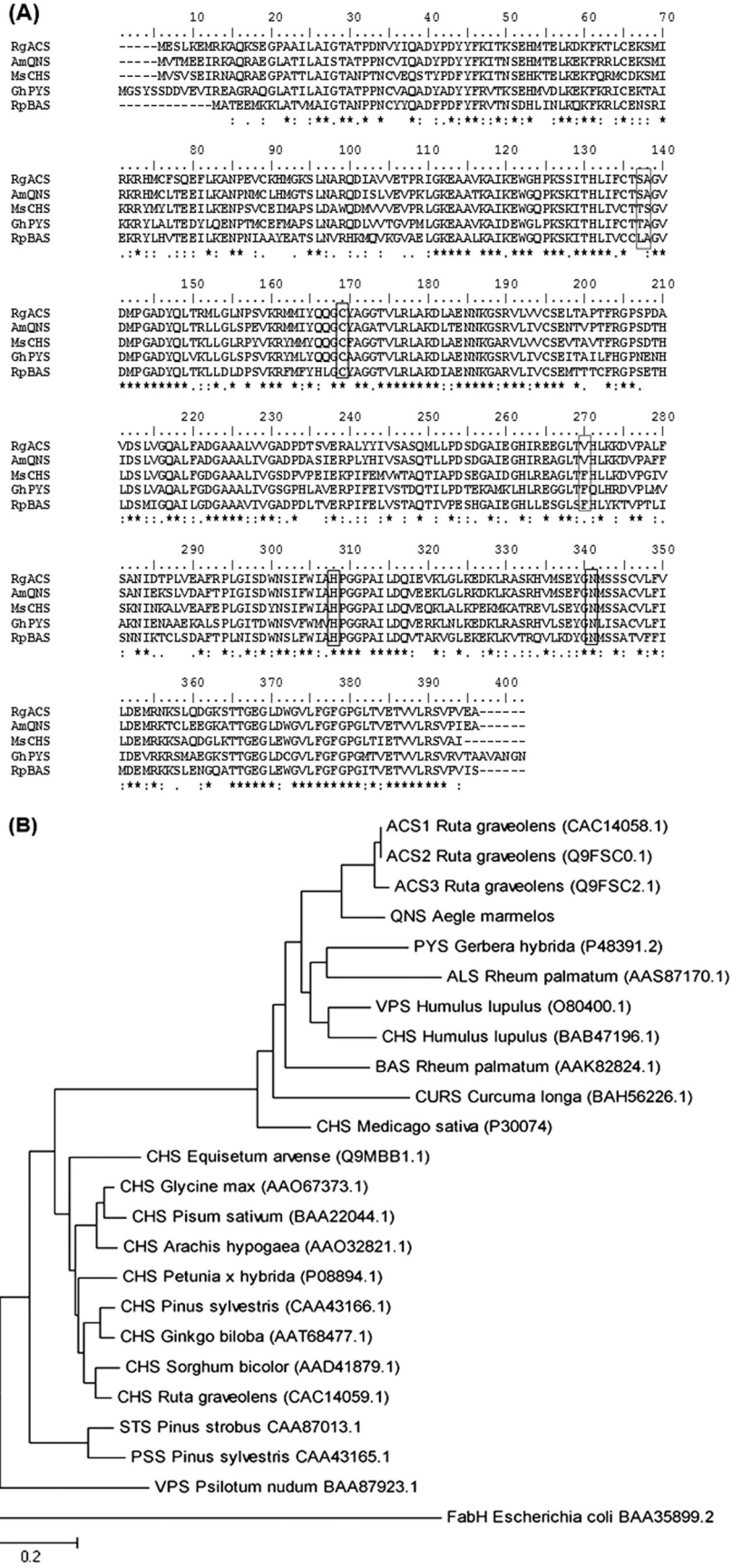
(A)
RgACS
AmQNS
MsCHS
GhPYS
RpBAS
(B)
ACS1 Ruta graveolens (CAC14058.1)
ACS2 Ruta graveolens (Q9FSC0.1)
ACS3 Ruta graveolens (Q9FSC2.1)
QNS Aegle marmelos
PYS Gerbera hybrida (P48391.2)
ALS Rheum palmatum (AAS87170.1)
VPS Humulus lupulus (O80400.1)
CHS Humulus lupulus (BAB47196.1)
BAS Rheum palmatum (AAK82824.1)
CURS Curcuma longa (BAH56226.1)
CHS Medicago sativa (P30074)
CHS Equisetum arvense (Q9MBB1.1)
CHS Glycine max (AAO67373.1)
CHS Pisum sativum (BAA22044.1)
CHS Arachis hypogaea (AAO32821.1)
CHS Petunia x hybrida (P08894.1)
CHS Pinus sylvestris (CAA43166.1)
CHS Ginkgo biloba (AAT68477.1)
CHS Sorghum bicolor (AAD41879.1)
CHS Ruta graveolens (CAC14059.1)
STS Pinus strobus CAA87013.1
PSS Pinus sylvestris CAA43165.1
VPS Psilotum nudum BAA87923.1
FabH Escherichia coli BAA35899.2
0.2

TABLE 1
Comparison of active site cavity residues of crystallized *M. sativa* CHS (Protein Data Bank code 1BI5) and *A. marmelos* QNS
The varied residues in QNS are underlined.

CHS *M. sativa*	QNS *A. marmelos*
Initiation pocket	
Leucine 214	Leucine 214
Isoleucine 254	Isoleucine 254
Glycine 256	Glycine 256
Phenylalanine 265	Valine 265
Elongation pocket	
Threonine 132	Serine 132
Serine 133	Alanine 133
Threonine 194	Threonine 194
Valine 196	Proline 196
Threonine 197	Threonine 197
Glycine 216	Alanine 216
Leucine 263	Leucine 263
Serine 338	Serine 338
Catalytic triad	
Cysteine 164	Cysteine 164
Histidine 303	Histidine 303
Asparagine 336	Asparagine 336

CoA and *p*-coumaroyl-CoA starter substrates were docked in the wild-type QNS and mutant substrate binding pocket. As expected, *N*-methylanthraniloyl-CoA and *p*-coumaroyl CoA starter substrates were finely docked into the active site cavities of QNS (Fig. 4). However, *N*-methylanthraniloyl-CoA, owing to steric clashes with both the substituted side chains residues, failed to dock in the active site pocket of both mutants, MSD1 and MSD2. Interestingly, *p*-coumaroyl-CoA finely docked in the substrate-binding pocket of the mutant proteins. Thus homology modeling studies suggest the crucial role of Ser-132 and Ala-133 in allowing binding of bulkier substrate as *N*-methylanthraniloyl-CoA (Fig. 4).

Wide Starter Substrate Specificity and Characterization of Novel Products—Due to the interesting results obtained by comparative modeling studies, we proceeded to biochemically characterize the QNS protein. The ability of QNS to accept various starter CoA with [2-^{14}C]malonyl-CoA as extender was investigated using Radio-TLC (Fig. 5). Several significant bands appear on the TLC plate, clearly indicating that QNS protein is able to accept various aromatic and small as well as bulky aliphatic substrates. Analogous broad starter substrate specificity has also been reported for other plant type III PKS (13). In support of our homology modeling and substrate binding studies of QNS that showed highest similarity with ACS, our radio-TLC analysis revealed a significant amount of product formation in the *N*-methylanthraniloyl-CoA-primed reaction. We decided to unambiguously characterize the nature of the product formed using nanospray electrospray ionization MS.

The major product shows R_f value similar to 4-hydroxy-1-methyl-2(1*H*)-quinolone standard. On MS analysis of the product, two molecular ion peak, $(M\text{-}H)^-$ at *m*/*z* 174.08 and $(M\text{-}H)^-$ at *m*/*z* 240.09 were observed. The structural elucidation of QNS reaction products was performed by using tandem mass spectrometry. Fig. 6*A* shows the fragmentation pattern for the molecular ion $(M\text{-}H)^-$ *m*/*z* 174.08 (obtained for a), which yielded a fragment of *m*/*z* 159.05 corresponding to ($C_9H_5NO_2$) (with the loss of −CH3 group), and *m*/*z* 131.05 corresponding to $(MCO_2\text{-}H)^-$ ion. This fragmentation pattern has been reported for the standard 4-hydroxy-1- methyl-2(1*H*)-quinolone also; which confirmed the formation of quinolone scaffold by QNS. Interestingly, the molecular ion peak $(M\text{-}H)^-$ at *m*/*z* 240.09 (obtained for b) yielded a fragment of *m*/*z* 225.06 corresponding to ($C_{13}H_8NO_3$) (with the loss of −CH3 group) and *m*/*z* 197.07 corresponding to $(MCO_2\text{-}H)^-$ ion (Fig. 6*B*), which were similar to the fragmentation pattern reported for 1,3-dihydroxy-*N*-methylacridone. The spectroscopic data (electrospray ionization MS and UV) of the compounds were characteristic of those of the quinolone and acridone and completely identical with those of authentic compounds and those cited in literatures. Thus, QNS may be a bifunctional enzyme capable of producing both quinolone and acridone *in vitro*. Because BAS is the only enzyme reported so far to produce quinolone scaffold whose physiological substrate is *p*-coumaroyl-CoA, we also tried to characterize the products biosynthesized by QNS protein with *p*-coumaroyl-CoA. Interestingly, the nanospray electrospray ionization MS analysis of the *p*-coumaroyl-CoA primed reaction showed a major molecular ion peak, $(M\text{-}H)^-$ at *m*/*z* 161.08 equivalent to *p*-hydroxybenzalacetone ($C_{10}H_{10}O_2$). Fig. 6*C* shows the fragmentation pattern for the molecular ion $(M\text{-}H)^-$ *m*/*z* 161.08 (obtained for c), which yielded a fragment of *m*/*z* 146.05 corresponding to ($C_9H_7O_2$) (with the loss of $-CH_3$ group) and *m*/*z* 119.06 corresponding to the $(MCO_2\text{-}H)^-$ ion. The products obtained with other substrates were similarly characterized by nanospray MS and determined to be triketide and tetraketide pyrones. With some notable exceptions (28, 29), the exclusive formation of pyrones by plant PKS seems to be an indicator that the starter CoA ester in the reaction is not the physiologically relevant substrate for the enzyme under assay (30). These findings suggest that pyrones produced by QNS *in vitro* might be derailment products due to non-physiological substrates or suboptimal reaction conditions.

Transformation of QNS to CHS by Site-directed Mutagenesis—From the sequence comparison and docking studies, it was observed that residues Ser-132 and Ala-133 line the substrate binding pocket of wild-type QNS (Fig. 3). Two mutant enzymes, a doublet (MSD1), in which the residues Ser-132 and Ala-133 were mutated to Thr-132 and Ser-133 and a triplet (MSD2), in which three residues, Ser-132, Ala-133 and Val-265 were mutated to Thr, Ser and Phe respectively were generated

FIGURE 2. **Alignment and phylogenetic analysis of QNS with other type III PKS.** *A*, alignment of QNS. The alignment was generated by CLUSTALW. *AmQNS*, *A. marmelos* quinolone synthase; *RgACS*, *R. graveolens* acridone synthase; *GhPYS*, *Gerbera hybrida* 2-pyrone synthase; *MsCHS*, *M. sativa* CHS2; *RpBAS*, *R. palmatum* benzalacetone synthase. The amino acids of the catalytic Cys-His-Asn triad are marked by *bold rectangular boxes*. The residues at positions Thr-132, Ser-133, and Phe-265 corresponding to *M. sativa* CHS (marked in *thin rectangular boxes*) in QNS have been shown to be lie near or line the active site cavity and Thr-132, Ser-133 are crucial for the binding of bulky starter substrate. The *stars below* each line of alignment indicates conserved sites. *B*, phylogenetic analysis of QNS with other type III PKS. The dendrogram was generated for *A. marmelos* QNS with other plant PKS. The accession numbers are given in *brackets*. *E. coli* ketoacyl synthase III (FabH) was used as an out group. *CHS*, chalcone synthase; *VPS*, valerophenone synthase; *ACS*, acridone synthase; *ALS*, aleosone synthase; *PYS*, pyrone synthase; *CURS*, curcuminoid synthase; *BLS*, benzalacetone synthase; *PSS*, pinosylvin synthase; *STS*, stilbene synthase.

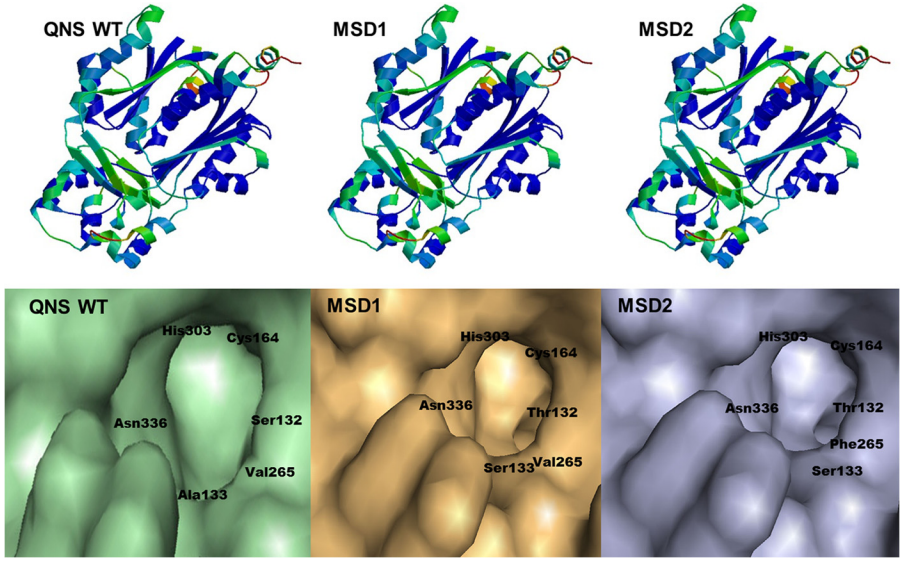

FIGURE 3. **Homology modeling and comparison of the active site cavities of *A. marmelos* QNS wild-type with mutant (MSD1 and MSD2) proteins.** Some of the crucial active site residues along with the catalytic triad Cys, His, and Asn are shown here.

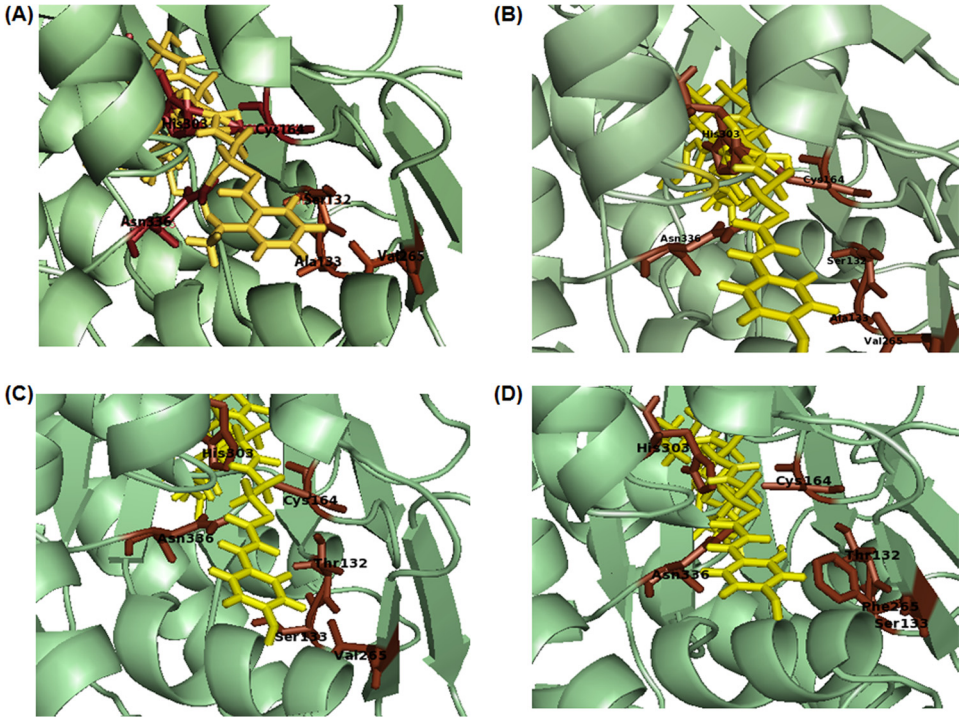

FIGURE 4. **Docking studies of QNS wild-type and mutant proteins, MSD1 and MSD2 with ligands.** *A*, QNS WT with *N*-methylanthraniloyl-CoA; *B*, QNS WT with *p*-coumaroyl-CoA; *C* and *D*, MSD1 (S132T/A133S) and MSD2 (S132T/A133S/V265F) with *p*-coumaroyl-CoA. Substrates were shown in *yellow*. Some of the crucial active site residues along with the catalytic triad Cys, His, and Asn were shown in *red*.

to gain an insight into the functional role of these residues. (MSD1 and MSD2 mutations were similar as generated for homology modeling studies.) QNS double and triple mutant homology model showed remarkable constriction in the active site cavity compared with wild-type QNS (Fig. 2). The steric hindrance was most probably due to the substitution of methyl group for hydrogen and charge substitution by the added hydroxyl group, thus occluding the chance of binding of bulky starter substrate in the substrate binding pocket of mutant enzyme. To validate our prediction, the QNS S132T/A133S and S132T/A133S/V265F mutants was heterologously overexpressed in *E. coli* as a recombinant protein with a His tag at the N terminus as in the case of wild-type QNS and purified to homogeneity by a nickel-chelate column. QNS S132T/A133S mutant (MSD1) exhibited chalcone-forming activity and performed sequential condensations of three malonyl-CoA units with *p*-coumaroyl-CoA to form tetraketide naringenin chalcone. The S132T/A133S/V265F triple mutant (MSD2), on the other hand, showed no product formation using *p*-coumaroyl-CoA as starter unit (Fig. 7). The production of naringenin chalcone by MSD1 was confirmed using authentic standard (R_f value, 0.8; retention time, 31.7). In support of our docking stud-

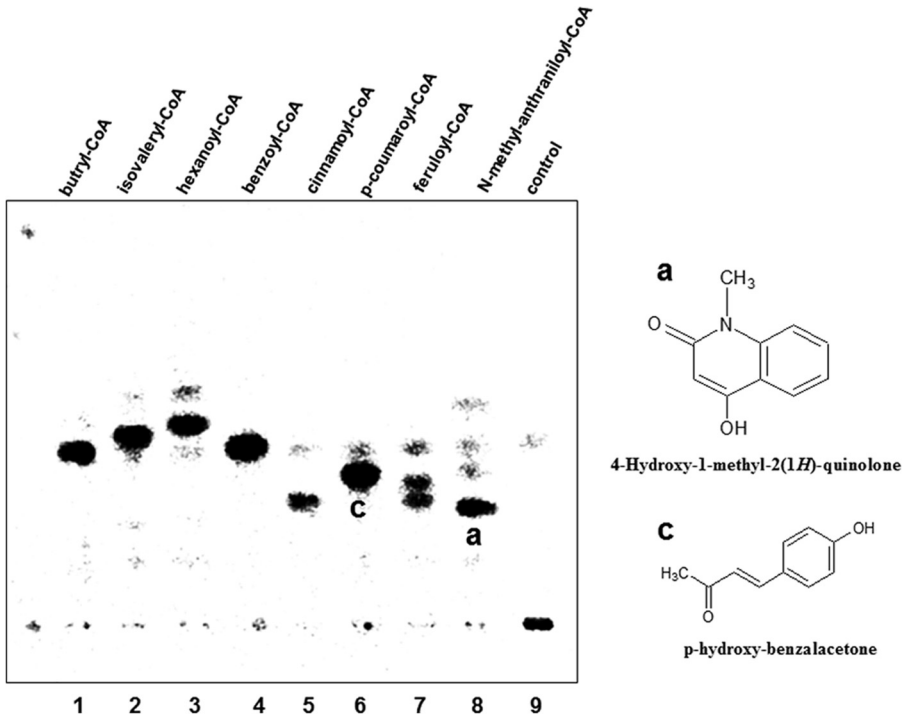

FIGURE 5. **TLC-based analysis of radiolabeled products of QNS wild-type.** The overall reaction was carried out by QNS with different substrate. Reactions were carried out for 2 h using [2-^{14}C]malonyl-CoA as an extender unit along with different starter substrates. The starter substrates used in the assay are indicated *above* each lane. Chemical structures of the major products obtained by *N*-methylanthraniloyl-CoA and *p*-coumaroyl-CoA primed reactions are indicated *next to* the radioactive bands. Because the R_f value of 1,3-dihydroxy-*N*-methylacridone was not known, it was not shown.

ies, none of the mutants formed products with *N*-methylanthraniloyl-CoA. Thus, the two amino acid substitution, S132T and A133S, which were predicted to line the QNS substrate binding pocket in the mutant MSD1, considerably shifted the starter substrate preference to *p*-coumaroyl-CoA and hence transformed the enzyme completely to a functional CHS producing naringenin (Fig. 7). Our results correlate with the reported transformation of ACS to CHS by triple mutation (27). The triple ACS mutant (S132T/A133S/V265F) retained ~35% ACS activity with an overall 10-fold increase in specific CHS activity. Interestingly, although the double mutant protein (S132T/A133S) displayed 100% CHS activity, the triple mutant showed no QNS/ACS/CHS activity, emphasizing a rather different enzyme mechanism.

Characterization of Kinetic Parameters of QNS—The starter unit specificity of QNS was investigated by performing steady state kinetic analysis using various CoA substrates. Type III PKS are generally known to possess broad substrate tolerance; we therefore performed kinetic studies with several different acyl-CoAs, the result of which was summarized in Table 2. Even though QNS produced aromatic products only with *N*-methylanthraniloyl-CoA and *p*-coumaroyl-CoA starter substrates, detailed kinetic studies were carried out with various starter CoAs, the result of which was summarized in Table 2. QNS displayed poor substrate affinity toward shorter aliphatic CoA thioesters and the benzoyl-, feruloyl-derived aromatic CoA-thioesters as reflected in the K_m values (Table 2). Hexanoyl-CoA and cinnamoyl-CoA were found to be efficient starter molecules for QNS, with k_{cat}/K_m values comparable with that of the physiological substrate. As reflected by the K_m values, the affinity of QNS for larger *N*-methylanthraniloyl-CoA starter was found to be higher compared with *p*-coumaroyl-CoA starter units. It can also be observed that the k_{cat}/K_m values for the biosynthesis of 4-hydroxy-1-methyl-quinolone are several folds higher than that observed for *p*-hydroxybenzalacetone (Table 2). For the formation of 4-hydroxy-1-methyl-quinolone, $K_m = 2.93\ \mu$M, $k_{cat} = 3.78\ min^{-1}$, $k_{cat}/K_m = 21{,}501.71\ M^{-1}\ s^{-1}$ for *N*-methylanthraniloyl-CoA and $K_m = 21.3\ \mu$M, $k_{cat} = 2.56\ min^{-1}$, $k_{cat}/K_m = 2003.13\ M^{-1}\ s^{-1}$) for extender malonyl-CoA. For *p*-hydroxybenzalacetone formation, the $K_m = 3.62\ \mu$M, $k_{cat} = 0.23\ min^{-1}$, $k_{cat}/K_m = 1{,}058.93\ M^{-1}\ s^{-1}$ for *p*-coumaroyl-CoA, and $K_m = 26.7\ \mu$M, $k_{cat} = 0.93\ min^{-1}$, $k_{cat}/K_m = 580.52\ M^{-1}\ s^{-1}$ for extender malonyl-CoA. *N*-Methylanthraniloyl-CoA is clearly the most preferred substrate *in vitro* and could also be the most preferred physiological starter substrate for QNS. To test whether the double mutant, MSD1, is biochemically relevant or not, we carried out a detailed kinetic studies for the double mutant (triple mutant, MSD2 is found to be biochemically non-functional and excluded from kinetic studies). As the double mutant showed activity only with *p*-coumaroyl-CoA, the same strater unit was used for kinetic analysis. For the mutant (MSD1) chalcone-forming reaction, the kinetic parameters for naringenin chalcone formation were $K_m = 3.43\ \mu$M, $k_{cat} = 2.14\ min^{-1}$, $k_{cat}/K_m = 10{,}398\ M^{-1}\ s^{-1}$) for *p*-coumaroyl-CoA and $K_m = 23.6\ \mu$M, $k_{cat} = 1.6\ min^{-1}$, $k_{cat}/K_m = 1129.94\ M^{-1}\ s^{-1}$) for extender malonyl-CoA. The mutant enzyme thus exhibited 10-fold increase in k_{cat}/K_m for *p*-coumaroyl-CoA as compared with the wild type QNS protein. Interestingly, MSD1 mutant showed rather narrow substrate tolerance and did not accept diverse starter substrates other than benzoyl-CoA.

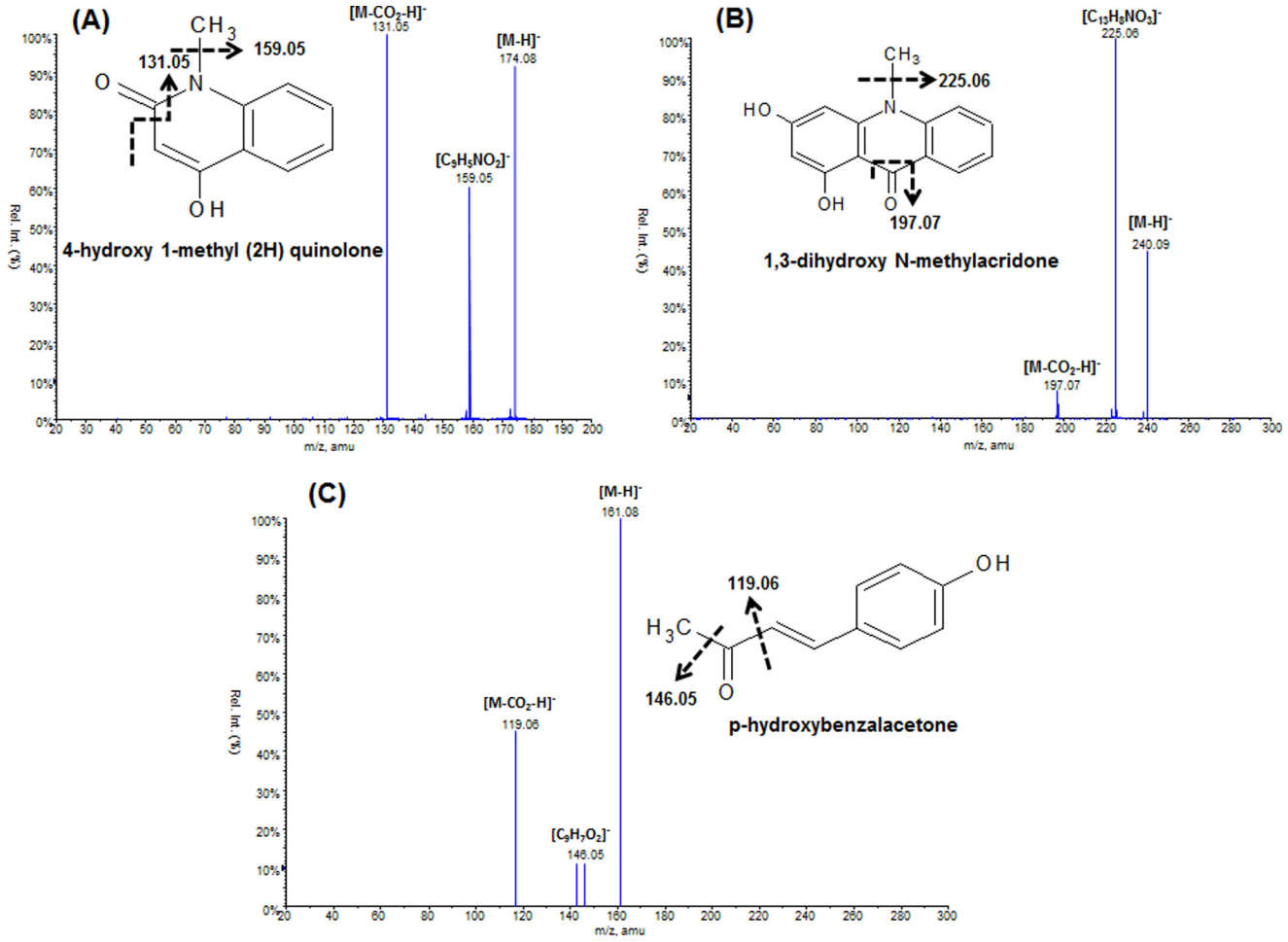

FIGURE 6. **Identification of QNS wild-type products.** The molecular mass obtained for each peak by nanospray mass spectrometric analysis is indicated *below* the structures for the expected products. *A* and *B* illustrate the fragmentation pattern observed by tandem mass spectrometry for *N*-methylanthraniloyl-CoA-primed products, 4-hydroxy-1-methyl-2(1*H*)-quinolone $(M-H)^-$ *m/z* 174.08 (*A*) and 1,3-dihydroxy-*N*-methylacridone $(M-H)^-$ *m/z* 240.09 (*B*). *C* illustrates the fragmentation pattern observed by tandem mass spectrometry for *p*-coumaroyl-CoA-primed product, *p*-hydroxybenzalacetone $(M-H)^-$ at *m/z* 161.08. Fragment ions are indicated *above* the corresponding peaks. The structure of the molecule with the expected fragmentation profile is drawn *next* to its MS/MS spectra. *Rel. Int.*, Relative Intensity.

DISCUSSION

The chemical diversity of alkaloids in the Rutaceae family has led to the isolation of various pharmacologically active natural products (31). Anthranilic acid has been postulated to be a key intermediate in the biosynthesis of various rutacean alkaloids, *viz.* quinolone and acridone alkaloids. Naturally occurring quinolones have profound medicinal properties and have served as lead structures for the design of synthetic quinolones as useful drugs (2). Although a number of functionally diverse type III PKS have been identified and characterized (13), no gene encoding for an enzyme catalyzing the formation of quinolone has yet been identified. Here, we report the identification of a novel type III PKS, QNS capable of catalyzing quinolone alkaloid biosynthesis from a rutacean member, *A. marmelos*. The overall reactions catalyzed by QNS protein is summarized in Fig. 8. In its native form, the QNS catalyzes the condensation of *N*-methylanthraniloyl-CoA with malonyl-CoA to form quinolone scaffold (major product, 89%) and acridone scaffold (minor product, 11%). QNS also shows significant BAS (benzalacetone) side activities in assays with *p*-coumaroyl-CoA. QNS also displays promiscuous substrate specificity *in vitro* by accepting both aliphatic and aromatic CoAs. Interestingly, CHS and other type III PKS, except ACS, do not accept the shorter and the bulkier *N*-methylanthraniloyl-CoA as a starter unit. Although the *M. sativa* CHS F215S mutant has been shown to accept *N*-methylanthraniloyl-CoA to produce an unnatural novel tetraketide lactone after three condensations with malonyl-CoA (14), it does not catalyze biosynthesis of acridone or quinolone.

R. graveolens ACS is the only type III PKS reported to be involved in rutacean alkaloid (acridone) biosynthesis (32). In ACS, the residues Ser-132, Ala-133, and Val-265 (numbering in *M. sativa* CHS) have been proposed to play a critical role for the selection of *N*-methylanthraniloyl-CoA as a starter substrate and for the formation of the acridone alkaloid. Indeed, an ACS triple mutant (S132T/A133S/V265F) has been shown to yield an enzyme that was functionally identical with CHS (27). A similar type of active site residue substitution in QNS prompted us to look into the role of these residues in substrate binding activity. Homology model and mutant studies of QNS showed that Ser-132 and Ala-133 residues to be involved in substrate binding, whereas Val-265 is occluded from starter substrate

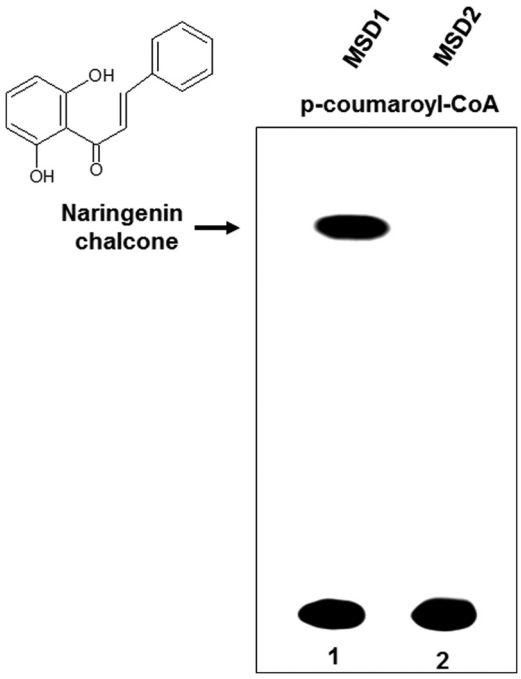

FIGURE 7. **Comparative TLC of radiolabeled products of QNS mutants, MSD1 (S132T/A133S) and MSD2 (S132T/A133S/V265F) of *p*-coumaroyl-CoA-primed reactions.** [2-^{14}C]Malonyl-CoA was used as an extender unit in both the reactions. Chemical structure of the major product obtained is indicated *next* to the radioactive band.

TABLE 2

Steady state kinetic parameters for QNS protein with different starter units

Results are means ($n = 3$) with S.E. values < 15%. ND, not determined.

Starter CoAs	k_{cat}	K_m	k_{cat}/K_m
	min^{-1}	μM	$s^{-1}{}_M{}^{-1}$
Butryl-CoA	ND	ND	ND
Isovaleryl-CoA	1.8	7.9	3797.47
Hexanoyl-CoA	2.53	4.2	10,039.68
Benzoyl-CoA	0.5	10.25	813.01
Cinnamoyl-CoA	2.9	5.2	9294.87
Feruloyl-CoA	1.12	9.14	2042.30
p-Coumaroyl-CoA	0.23	3.62	1058.93
N-Methylanthraniloyl- CoA	3.78	2.93	21,501.71

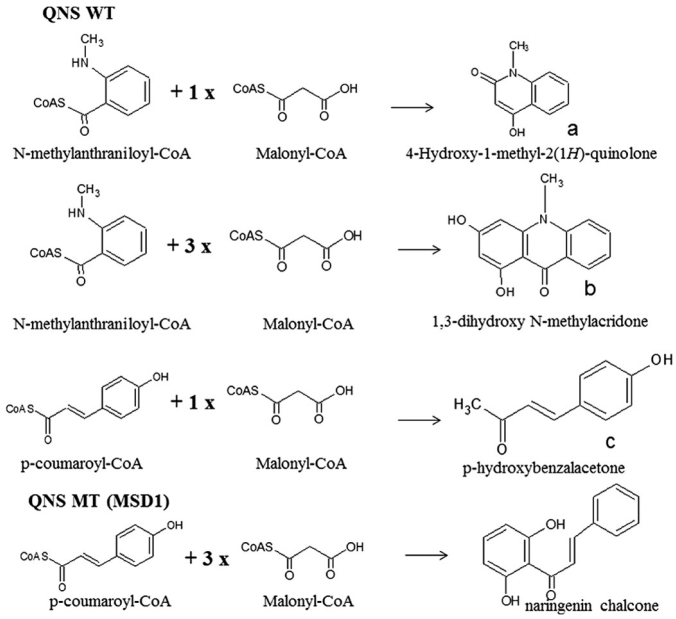

FIGURE 8. **Overall reactions catalyzed by *A. marmelos* QNS wild-type and mutant, MSD1.**

binding. These amino acids line the active site cavity of QNS and are not conserved in other members of the PKS family other than ACS. In accordance with our docking studies the functional behavior of QNS was dramatically altered in the mutant, MSD1, where S132T/A133S substitution in the active site cavity transformed QNS completely into CHS. Substitution of Ser-132 to Thr and Ala-133 to Ser had dual effects on enzyme activity. First, the double mutant completely lost the ability to accept *N*-methylanthraniloyl-CoA. Secondly, the mutant showed an overall increase in polyketide chain elongation. This could be explained by the constriction of the active site cavity by the introduction of methyl group in the Thr residue, thus excluding larger substrates in active site pocket. In *Aloe arborescens* pentaketide chromone synthase, a point mutation, M207G, expanded the volume of cavity, thereby converting pentaketide chromone synthase into octaketide synthase (33). Compared with the substrate cavity of wild-type QNS, the size of the accessible pocket in MSD1 and MSD2 is smaller and does not allow the binding of bulky starter substrate such as *N*-methylanthraniloyl-CoA, thereby preventing the formation of quinolone or acridone. The docking studies with double and triple mutant confirm the complete exclusion of *N*-methylanthraniloyl-CoA from substrate binding pocket. Although the double mutant protein (MSD1) displayed 100% CHS activity with *p*-coumaroyl-CoA, showing no QNS side activity with *N*-methylanthraniloyl-CoA, the triple mutant purified enzyme (MSD2), when incubated with both starter CoAs, was not able to produce any significant bands in the radio-TLC. It was rather surprising because similar triple mutant generated for acridone synthase were reported to be 100% functional producing naringenin chalcone with *p*-coumaroyl-CoA (27). The mutations, in particular, in MSD1 must have significantly altered the space and/or charge restrictions of the active site pocket, and the difference in geometry caused the change in the starter substrate preference. The shape and volume of the active site cavity greatly influence the substrate specificity and control the final length of the polyketide (34). Replacement of the S132T and A133S may open the gate to a buried pocket, into which the triketide intermediate is redirected during the elongation process of the diketide. It was thus confirmed that the residues S132T and A133S in *A. marmelos* QNS are indeed involved in the formation of quinolone and that the preference toward increased polyketide chain extension at the diketide stage in the mutant was due to the absence of these residues. A combination of three mutations (T197L/G256L/S338I) converted *M. sativa* CHS into 2-pyrone synthase by reducing the volume of the active site cavity from 923 to 274 Å^3 (34). The T135L point mutation not only changed the product specificity but also the substrate specificity of BPS, thus transforming it into a functional phenylpyrone synthase (35).

BAS, a member of the type III PKS superfamily from *Rheum palmatum*, which catalyzes a one-step decarboxylative condensation of *p*-coumaroyl-CoA with malonyl-CoA to produce *p*-hydroxybenzalacetone is the only reported enzyme capable

of enzymatic synthesis of quinolone derivatives (10). Because quinolone alkaloids have never been isolated from *R. palmatum* (Polygonaceae) and are completely or largely restricted to Rutaceae, the physiological role of BAS in quinolone alkaloid biosynthesis still remains obscure. The identified QNS from *A. marmelos*, a rutacean member rich in quinolone and acridone alkaloid derivatives, is a more physiologically relevant novel potential type III PKS catalyzing quinolone scaffold biosynthesis. As mentioned previously, QNS double mutant (S132T/A133S) yield an enzyme that was functionally identical with CHS, whereas triple mutant fail to produce quinolone or acridone or naringenin. However, two of the mentioned residues, Ser-132 and Ala-133 are not conserved in *R. palmatum* BAS that accepted the anthraniloyl starter; instead, it was S132L/V265F. One of the most unique features of *R. palmatum* BAS is that it lacks active site Phe-215; the conserved residues Ile214Leu. Interestingly, the diketide-forming activity of the BAS enzyme is reported to be derived from the characteristic substitution of the active site gatekeeper Phe-215 by Leu (10). A BAS I214L/L215F mutant exhibited chalcone-forming activity, which also supported a hypothesis that the absence of Phe-215 in BAS accounts for the interruption of the polyketide chain elongation at the diketide stage (36). Even though QNS also showed considerable benzalacetone side activity with *p*-coumaroyl-CoA, Phe-215 is well conserved in QNS similar to all other type III PKS.

In addition to the diketide condensation, wild-type QNS shows a minor tetraketide condensation leading to the formation of acridone such as ACS. ACS and CHS catalyze similar condensation reactions up to the tetraketide stage, but subtle differences exist in the modes of cyclization. The final bridging of rings in acridone biosynthesis must formally precede from a non-aromatic "trione" intermediate (37) proceeds through nucleophilic substitution followed by dehydration. In contrast, CHS releases the chalcone as the immediate product, which in the absence of chalcone isomerase, cyclizes non-stereoselectively to the flavanone naringenin. Although QNS is also capable of similar type of condensation reaction up to the tetraketide stage releasing acridone scaffold, under most of the experimental tests conducted, it favors interruption of the chain extension at the diketide stage, releasing quinolone scaffold. QNS preference toward single condensation is well shown with *p*-coumaroyl substrate also, by catalyzing a one-step decarboxylative condensation with malonyl-CoA to produce a diketide benzalacetone. The BAS is reported to carry out only one condensation with *N*-methylanthraniloyl-CoA and methylmalonyl-CoA to produce quinolone scaffold, even though it can easily carry out two condensation reaction with *p*-coumaroyl-CoA (10). The results support a different type of reaction mechanism for QNS.

Kinetic characterization of QNS and MSD1 demonstrated that the S132T/A133S mutation results in increased affinity for the starter substrate, *p*-coumaroyl-CoA, and increased turnover number resulting in an overall increased catalytic efficiencies (k_{cat}/K_m). Steady-state enzyme kinetics for the formation of 4-hydroxy-1,3-dimethyl-2(1*H*)-quinolone by reported BAS is K_m of 23.7 μM and k_{cat} of 1.48 min^{-1} for *N*-methylanthraniloyl-CoA, whereas for QNS these are 2.93 μM and 3.8 min^{-1}, respectively. For the formation of benzalacetone, the normal product of the BAS enzyme is K_m of 10.0 μM and k_{cat} of 1.79 for *p*-coumaroyl-CoA (25) and for QNS, 3.62 μM and 0.23 min^{-1}, respectively. The severalfold increase in affinity of QNS for *N*-methylanthraniloyl-CoA and overall increased catalytic efficiency for quinolone formation in comparison with BAS suggests its physiological preference toward quinolone biosynthesis.

In conclusion, we have characterized a novel type III PKS protein that catalyzes the formation of quinolones using bulky acyl-CoA substrates. Structural and mutational studies have suggested that QNS might have emerged by the gain of function mutation (by the substitution of simply two active site residues) from a structurally homologous CHS type III protein. The functional equivalence of mutant QNS to CHS proteins rather presents a fascinating evolutionary link. Furthermore, recent structure-based engineering of functionally divergent type III PKS has significantly expanded the catalytic repertoire of the enzymes and the product diversity (38–40). The identified PKS (QNS) due to its unusual substrate specificity and with its ability to produce quinolone scaffold can be utilized for the production of chemically and structurally distinct unnatural novel alkaloids.

REFERENCES

1. Michael, J. P. (2008) Quinoline, quinazoline and acridone alkaloids. *Nat. Prod. Rep.* **25,** 166–187
2. Heeb, S., Fletcher, M. P., Chhabra, S. R., Diggle, S. P., Williams, P., and Cámara, M. (2011) Quinolones: from antibiotics to autoinducers. *FEMS Microbiol. Rev.* **35,** 247–274
3. Robert, A., and Meunier, B. (1998) Is alkylation the main mechanism of action of the antimalarial drug artemisinin? *Chem. Soc. Rev.* **27,** 273–274
4. Alhaider, A. A., Abdelkader, M. A., and Lien, E. J. (1985) Design, synthesis, and pharmacological activities of 2-substituted 4-phenyl quinolines as potential antidepressant drugs. *J. Med. Chem.* **28,** 1394–1398
5. Cheng, J. T. (1986) Effect of skimmianine on animal behavior. *Arch. Int. Pharmacodyn. Ther.* **281,** 35–43
6. Cheng, J. T., Chang, S. S., Chen, I. S. (1990) Cardiovascular effect of skimmianine in rats. *Arch. Int. Pharmacodyn. Ther.* **306,** 65–74
7. Chen, K. S., Chang, Y. L., Teng, C. M., Chen, C. F., and Wu, Y. C. (2000) Furoquinolines with antiplatelet aggregation activity from leaves of *Melicope confusa*. *Planta Med.* **66,** 80–81
8. Jansen, O., Akhmedjanova, V., Angenot, L., Balansard, G., Chariot, A., Ollivier, E., Tits M., and Frédérich, M. (2006) Screening of 14 alkaloids isolated from Haplophyllum A *Juss.* for their cytotoxic properties. *J. Ethnopharmacol.* **105,** 241–245
9. Cheng, J. T., Chang, T. K., and Chen, I. S. (1994) Skimmianine and related furoquinolines function as antagonists of 5-hydroxytryptamine receptors in animals. *J. Auton. Pharmacol.* **14,** 365–374
10. Abe, I., Abe, T., Wanibuchi, K., and Noguchi, H. (2006) Enzymatic formation of quinolone alkaloids by a plant type III polyketide synthase. *Org. Lett.* **8,** 6063–6065
11. Nugroho, A. E., Riyanto, S., Sukari, M. A., and Maeyamad, K. (2010) Effects of skimmianine, a quinolone alkaloid of *Aegle marmelos* Correa roots, on the histamine release from rat mast cells. *J. Basic Appl. Sci.* **6,** 141–148
12. Riyanto, S., Sukari, M. A., Rahmani, M., Ee, G. C. L., Yap, Y. H. T., Aimi, N., Kitajima, M. (2001) Alkaloids from *Aegle marmelos* (Rutaceae). *Malays. J. Analy. Sci.* **7,** 463–465
13. Austin, M. B., and Noel, J. P. (2003) The chalcone synthase superfamily of type III polyketide synthases. *Nat. Prod. Rep.* **20,** 79–110
14. Jez, J. M., Bowman, M. E., and Noel, J. P. (2002) Expanding the biosynthetic repertoire of plant type III polyketide synthases by altering starter molecule specificity. *Proc. Natl. Acad. Sci. U.S.A.* **99,** 5319–5324
15. Ghosh, R., Chhabra, A., Phatale, P. A., Samrat, S. K., Sharma, J., Gosain, A., Mohanty, D., Saran, S., and Gokhale, R. S. (2008) Dissecting the functional

role of polyketide synthases in *Dictyostelium discoideum*: biosynthesis of the differentiation regulating factor 4-methyl-5-pentylbenzene-1,3-diol. *J. Biol. Chem.* **283,** 11348–11354
16. Saxena, P., Yadav, G., Mohanty, D., and Gokhale, R. S. (2003) A new family of type III polyketide synthases in *Mycobacterium tuberculosis*. *J. Biol. Chem.* **278,** 44780–44790
17. Arnold, K., Bordoli, L., Kopp, J., and Schwede, T. (2006) The SWISS-MODEL workspace: a web-based environment for protein structure homology modelling. *Bioinformatics* **22,** 195–201
18. Kiefer, F., Arnold, K., Künzli, M., Bordoli, L., and Schwede, T. (2009) The SWISS-MODEL Repository and associated resources. *Nucleic Acids Res.* **37,** D387–92
19. Peitsch, M. C. (1995) Protein modeling by E-mail Bio/Technology. *Nat. Biotechnol.* **13,** 658–660
20. Liang, J., Edelsbrunner, H., Woodward, C. (1998) Anatomy of protein pockets and cavities: Measurement of binding site geometry and implications for ligand design. *Protein Sci.* **7,** 1884–1897
21. Ritchie, D. W., and Kemp, G. J. (2000) Protein docking using spherical polar Fourier correlations. *Proteins* **39,** 178–194
22. Durbin, M. L., McCaig, B., and Clegg, M. T. (2000) Molecular evolution of the chalcone synthase multigene family in the morning glory genome. *Plant Mol. Biol.* **42,** 79–92
23. Schroder, J. (1997) A family of plant-specific polyketide synthases: Facts and predictions. *Trends Plant Sci.* **2,** 373–378
24. Zheng, D., Schröder, G., Schröder, J., and Hrazdina, G. (2001) Molecular and biochemical characterization of three aromatic polyketide synthase genes from Rubus idaeus. *Plant Mol. Biol.* **46,** 1–15
25. Abe, I., Takahashi, Y., Morita, H., Noguchi, H. (2001) Benzalacetone synthase. A novel polyketide synthase that plays a crucial role in the biosynthesis of phenylbutanones in *Rheum palmatum*. *Eur. J. Biochem.* **268,** 3354–3359
26. Resmi, M. S., and Soniya, E. V. (2012) Molecular cloning and differential expressions of two cDNA encoding Type III polyketide synthase in different tissues of *Curcuma longa* L. *Gene* **491,** 278–283
27. Lukacin, R., Schreiner, S., and Matern, U. (2001) Transformation of acridone synthase to chalcone synthase. *FEBS Lett.* **508,** 413–417
28. Akiyama, T., Shibuya, M., Liu, H. M., and Ebizuka, Y. (1999) p-Coumaroyl triaceticacid synthase, a new homologue of chalcone synthase, from *Hydrangea macrophylla* var. thunbergii. *Eur. J. Biochem.* **263,** 834–839
29. Eckermann, S., Schroder, G., Schmidt, J., Strack, D., Edrada, R. A., Helariutta, Y., Elomaa, P., Kotilainen, M., Kilpelainen, I., Proksch, P., Teeri, T. H., and Schroder, J. (1998) New pathway to polyketides in plants. *Nature* **396,** 387–390
30. Samappito, S., Page, J. E., Schmidt, J., De-Eknamkul, W., and Kutchan, T. M. (2003) Aromatic and pyrone polyketides synthesized by a stilbene synthase from Rheum tataricum. *Phytochemistry* **62,** 313–323
31. Tillequin, F. (2007) Rutaceous alkaloids as models for the design of novel antitumor drugs. *Phytochem. Rev.* **6,** 65–79
32. Junghanns, K. T., Kneusel, R. E., Baumert, A., Maier, W., Gröger, D., and Matern, U. (1995) Molecular cloning and heterologous expression of acridone synthase from elicited *Ruta graveolens* L. cell suspension cultures. *Plant Mol. Biol.* **27,** 681–692
33. Morita, H., Kondo, S., Oguro, S., Noguchi, H., Sugio, S., Abe, I., and Kohno, T. (2007) Structural insight into chain-length control and product specificity of pentaketide chromone synthase from *Aloe arborescens*. *Chem. Biol.* **14,** 359–369
34. Jez, J. M., Austin, M. B., Ferrer, J., Bowman, M. E., Schröder, J., Noel, J. P. (2000) Structural control of polyketide formation in plant-specific polyketide synthases. *Chem. Biol.* **7,** 919–930
35. Klundt, T., Bocola, M., Lütge, M., Beuerle, T., Liu, B., and Beerhues, L. (2009) A Single Amino Acid Substitution Converts Benzophenone Synthase into Phenylpyrone Synthase. *J. Biol. Chem.* **284,** 30957–30964
36. Abe, I., Sano, Y., Takahashi, Y., and Noguchi, H. (2003) Site-directed mutagenesis of benzalacetone synthase. The role of the Phe215 in plant type III polyketide synthases. *J. Biol. Chem.* **278,** 25218–25226
37. Dewick, P. M. (1997) Medicinal Natural Products. A Biosynthetic Approach, pp. 123–124, Wiley, New York
38. Abe, I., Watanabe, T., Morita, H., Kohno, T., Noguchi, H. (2006) Engineered biosynthesis of plant polyketides: manipulation of chalcone synthase. *Org. Lett.* **8,** 499–502
39. Shi, S. P., Wanibuchi, K., Morita, H., Endo, K., Noguchi, H., and Abe, I. (2009) Enzymatic formation of unnatural novel chalcone, stilbene, and benzophenone scaffolds by plant type III polyketide synthase. *Org. Lett.* **11,** 551–554
40. Morita, H., Yamashita, M., Shi, S. P., Wakimoto, T., Kondo, S., Kato, R., Sugio, S., Kohno, T., and Abe, I. (2011) Synthesis of unnatural alkaloid scaffolds by exploiting plant polyketide synthase. *Proc. Natl. Acad. Sci. U.S.A.* **108,** 13504–13509